Materials Science-Poland, 35(4), 2017, pp. 733-745
http://www.materialsscience.pwr.wroc.pl/
DOI: 10.1515/msp-2017-0094

DE GRUYTER OPEN

Magnetic characterization of microcrystalline $Na_3Ln_{0.99-x}Er_{0.01}Cr_x(PO_4)_2$ orthophosphates synthesized by Pechini method (Ln = La, Gd)

S.M. KACZMAREK[1,*], G. LENIEC[1], H. FUKS[1], T. SKIBIŃSKI[1], A. PELCZARSKA[2], P. GODLEWSKA[2], J. HANUZA[2,3], I. SZCZYGIEŁ[2]

[1]Institute of Physics, Faculty of Mechanical Engineering and Mechatronics, Westpomeranian University of Technology In Szczecin, Al. Piastów 19, 70-310 Szczecin, Poland

[2]Wrocław University of Economics, Faculty of Chemistry and Food Technology, ul. Komandorska 118/120, 53-345 Wrocław, Poland

[3]Institute of Low Temperature and Structure Research, Polish Academy of Sciences, ul. Okólna 2, 50-422 Wrocław, Poland

$Na_3Ln(PO_4)_2$ orthophosphates (Ln = La, Gd) doped with Er^{3+} and co-doped with Cr^{3+} ions were synthesized by Pechini method and characterized by electron paramagnetic resonance (EPR) and magnetic susceptibility measurements. Low temperature EPR spectra were detected and analyzed in terms of temperature dependence and the structure of the obtained materials. They show that erbium and chromium ions substitute Ln^{3+} and also Na^+ ions or Na^+ channels forming complex EPR spectra. Both kinds of ions reveal ferromagnetic type of interaction which shows some anomaly at the temperature between 10 K and 15 K. Magnetic susceptibility reveals a weak antiferromagnetic kind of interaction dominating in the whole temperature range, from 3.5 to 300 K.

Keywords: *orthophosphates; erbium; chromium; EPR technique, magnetization measurements*

1. Introduction

Various lanthanide phosphates have been a subject of extensive structural and spectroscopic studies due to their important optical properties [1–12]. They exhibit a good chemical and thermal stability and optical efficiency. Therefore, they are applied as green light emitters in fluorescent lamps when doped with terbium [13] or mini-lasers when doped with neodymium [14]. Recently, a new approach to well known materials has been applied since the discovery of unique properties of nanoceramics obtained by high-pressure technique [15]. The phosphates of the $M_3RE(PO_4)_2$ composition, where M = Na, K or Rb, RE – a rare-earth element – belong to glaserite-type structure compounds and are characterized by rich polymorphism. Moore [16] introduced a bracelet and pinwheel description for glaserite-like sulfates. Applying this approach to glaserite-type double phosphates, the pinwheel or the structural subunit is formed by $[REO_6]$ octahedron that shares its six corners with $[PO_4]$ tetrahedron that alternates "up" and "down." The pinwheels are linked through $[PO_4]$ tetrahedra to form layers with alkali atoms located between the layers. Depending on the radius of RE ion its coordination may increase to seven/eight and the symmetry may be lowered (from hexagonal to monoclinic). Their structural and optical properties have been studied in detail [16–30]. Main orthorhombic forms of sodium orthophosphates $Na_3RE(PO_4)_2$ have been optically characterized [8, 18–20, 24, 30]. The phosphates doped with various active ions could be easily obtained and commercially used. In a previous paper, we described Pechini method of synthesis as well as the thermal behavior and properties of sub-microcrystalline Yb^{3+}-doped $Na_3RE(PO_4)_2$ orthophosphates, where RE = La, Gd, Y [31].

*E-mail: skaczmarek@zut.edu.pl

Their structure, vibrational, optical absorption and emission spectra were analyzed and possible applications of the studied orthophosphates were discussed. To find possible sites occupied by rare-earth or transition metal ions it is worth doping $Na_3RE(PO_4)_2$ with, e.g. two agents. Erbium ion is interesting due to its luminescence properties, chromium ion could be a probe. The basic features of Cr^{3+} in a number of crystalline solids are established so well that Cr^{3+} is frequently used as a probe to study the structure and the local symmetry of new materials. In the present paper we describe EPR and magnetic susceptibility measurements of erbium doped and chromium co-doped lanthanum and gadolinium orthophosphates. Magnetic properties of the compounds have been analyzed and discussed in terms of lattice positions of incorporated dopants and the structure of these materials. They are strongly dependent on Ln^{3+} cations.

2. Experimental

$Na_3Ln_{0.99-x}Er_{0.01}Cr_x(PO_4)_2$ phosphates of the composition Ln = La, Gd; x = 0.001 to 0.004 were prepared by a modified Pechini process [32]. A detailed description of the synthesis was presented in the literature [31]. After the synthesis all the samples were calcined at 700 °C for 1 h. Annealing of the obtained orthophosphates at 700 °C led to grains of ~200 nm. The detailed crystal structure of $Na_3La(PO_4)_2$ is not known. Some similarity of this structure to that of $Na_3Ce(PO_4)_2$ has only been suggested. The latter compound adopts the orthorhombic space group $Pca2_1$ (C^5_{2v}) structure with the lattice parameters of about: a = 14.1, b = 5.4 and c = 18.7 Å, Z = 8 [33]. In this structure, each Na^+ ion is surrounded by six Na^+ and two Ce^{3+} ions. Each Ce^{3+} ion has eight sodium ions in its neighborhood. Ce^{3+} ions occupy the sites of the general C_1 symmetry, and can be substituted by doping ions (Fig. 1a).

Sodium gadolinium phosphate, $Na_3Gd(PO_4)_2$, has been obtained in different crystal structures: trigonal, tetragonal, orthorhombic and monoclinic. One of the monoclinic modifications was refined in the space group C2/c (Z = 12) with the unit cell parameters of about: a = 27.5 Å, b = 5.3 Å, c = 13.9 Å, β = 91.3°, V = 2039 Å^3 [12]. This structure is built by three-dimensional $GdP_2O_8^{3-}$ anionic framework with two different types of internal tunnels incorporating Na atoms (C_1 and C_i site symmetry). Isolated PO_4 tetrahedra (C_1 site symmetry), and two types GdO_8 and GdO_7 polyhedra (C_i and C_1 site symmetries) build this framework. The Gd–Gd distances in the unit cell lie in the range of 4.742 Å to 6.458 Å. In such a structure Er^{3+} and Cr^{3+} ions can substitute the Gd-sites as well as tunnels occupied by Na^+ ions (Fig. 1b).

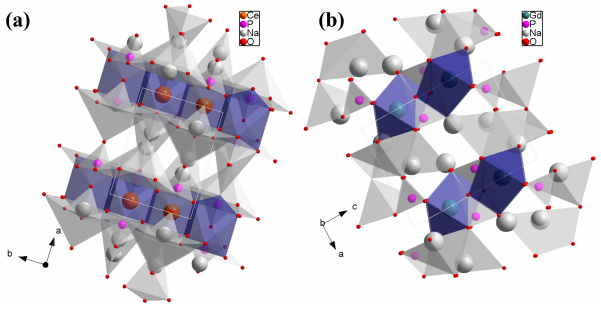

Fig. 1. Crystal structure of (a) $Na_3Ce(PO_4)_2$ [33] and (b) $Na_3Gd(PO_4)_2$ [12].

The first derivative of the powder absorption spectra was recorded as a function of an applied magnetic field on a conventional X-band Bruker ELEXSYS E 500 CW spectrometer operating at 9.5 GHz with 100 kHz magnetic field modulation. Temperature dependences of EPR spectra of the samples were recorded using an Oxford Instruments ESP helium-flow cryostat.

The static (DC) magnetic susceptibility measurements were performed using a Quantum Design MPMS XL–7 with EverCool Magnetic Property Measurement System. The measurements were performed at temperature up to 305 K and magnetic field in the range H = 100 Oe to 10.000 Oe. DC susceptibilities were measured in the zero-field-cooling (ZFC) and field-cooling (FC) modes.

3. Magnetic properties of $Na_3La_{0.99-x}Er_{0.01}Cr_x(PO_4)_2$: x = 0.001 to 0.004

3.1. EPR results

Powder samples of $Na_3La(PO_4)_2$:1 mol% Er, 0.1 to 0.4 mol% Cr compounds were investigated using EPR technique. The X-band resonance spectra registered at temperature 3.5 K to 300 K revealed the presence of a complex signal in the wide magnetic resonance field range (Fig. 2a for chromium concentration 0.1 to 0.4 mol%). In the next part of our paper, due to higher resolution of EPR spectrum, we focused our attention on the EPR analysis of $Na_3La(PO_4)_2$:1 mol% Er, 0.4 mol% Cr sample. Nonuniform intensity, asymmetric shape and a large width of the resonance lines allow us to conclude that different magnetic centers are responsible for the observed EPR signal. Indeed, taking into consideration temperature behavior of the EPR signal (Fig. 2b) we divided the whole resonance signal into three different parts: (a) a low field signal observed at magnetic field below 100 mT, ascribed to Er^{3+} ions at lanthanum lattice positions, (b) a group of lines centered at about 330 mT, with $g_{eff} \approx 1.99$, ascribed to chromium ions at lanthanum or sodium lattice positions, gadolinium uncontrolled dopant and to a signal originating from a quartz pipe, and (c) a resonance line visible at magnetic field close to 1000 mT, also assigned to Cr^{3+} ions. The EPR signal centered at ~1200 mT, observed in Fig. 2, has an external meaning (oxygen) and has not been taken into consideration. Moreover, it is not excluded that a broad band at $g \sim 2$ is an effect of Cr^{3+}–Cr^{3+}/Na^+ pairs interaction [34].

Paramagnetic Er^{3+} ions can be visible in the EPR spectra at low temperature (<30 K) and low magnetic field. Erbium in a powder compound has an effective spin S = 1/2 and its EPR spectrum mainly contains one narrow and asymmetric line.

EPR signals originating from Cr^{3+} ions (S = 3/2) can be observed up to room temperature and in a wide range of magnetic field. Isolated chromium ions give an EPR signal centred at $g \sim 2$ (a large distortion in an axial symmetry can split the EPR signal shifting it towards lower magnetic fields, up to $g \sim 3.74$ [35]), chromium pairs above $g > 2$, and, other ions pairs, such as Er^{3+}–Na^+ or Cr^{3+}–Na^+ below $g < 2$ [34]. The EPR signal of chromium ions with a spin of S = 3/2 is composed of three separate and narrow lines with relatively low intensity.

After subtraction of the signal originating from a quartz pipe from the overall EPR signal, deconvolution of the signal centered at about 330 mT (Fig. 3a, T = 3.5 K) allowed us to find that the group of lines is composed of at least three lines (262, 336 and 421 mT) that we assigned to Cr^{3+} isolated ion (chromium site No. 1, $g_{eff} \sim 1.99$). This site is more probably assigned to lanthanum octahedral positions. Moreover, additional lines, centered at 176 mT, 300 mT and 951 mT, which have been identified, we assigned to the second kind of isolated chromium center (chromium site No. 2, $g \sim 3.74$). The latter site differs significantly from the former by values of zero field splitting parameters (D, E). D parameter calculated for this site takes huge value as compared to the corresponding value calculated for chromium site No. 1. D parameter indicates a scale of distortion of local environment of paramagnetic ions. Chromium ions in the sites seem to be isolated Cr^{3+} ions experiencing low symmetry crystal field [36]. We assigned the sites to sodium or interstitial positions. Both chromium sites we ascribed to chromium ions with a spin of S = 3/2. A simulation performed using EPR-NMR program [37] excluded the presence of pairs in the investigated compounds. From the simulation we obtained the following parameters: chromium center (1): S = 3/2, $g_x = 1.98$, $g_y = 1.99$, $g_z = 2.02$, E = 0, $D = 825 \times 10^{-4}$ cm^{-1}, $g_{eff} = 1.99$, chromium center (2): S = 3/2, $g_x = 2.01$, $g_y = 1.99$, $g_z = 2.05$, $E = 50 \cdot 10^{-4}$ cm^{-1}, $D = 10.950 \times 10^{-4}$ cm^{-1}, $g_{eff} = 1.99$. As one can see, the D zero field splitting parameter reaches ~1.1 cm^{-1} for chromium center (2), which is an unusual value for chromium centers observed in solids. It usually adopts value as high as 0.03 cm^{-1}, as e.g. for ammonium dihydrogen phosphate doped

with Cr^{3+} [38]. But there are some crystals revealing larger values of D parameter. $Bi_4Ge_3O_{12}$: Cr reveals D = 0.967 cm^{-1} [39], while Mg_2SiO_4:Cr reveals D ~ 2 cm^{-1} [40]. From Fig. 3a one can see that the ratio of the EPR amplitudes for both sites is as high as 2, which indicates that twice as many chromium ions occupy center (1) than center (2).

In addition to the two paramagnetic centers, we were able to recognize free electrons line of Dyson-like shape, centered at g ~ 2, resulting from charge compensation of sodium ion substitution for chromium one. In Fig. 3a we presented all the centers giving contribution to an overall EPR spectrum, taking also into account the EPR signal from isolated Er^{3+} ions, centered at about 56 mT, g ~ 12. The simulation made by using EPR-NMR program gave the following parameters for erbium ions: S = 1/2, g_x = 13.5, g_y = 11.9, g_z ~ 2. As one can see, the g values indicate a large magnetic anisotropy and low local symmetry of erbium ions. Due to distinct difference between g_x and g_y values, we suppose that this is the case when coordination number of Er^{3+} ions changes to seven/eight, although they substitute lanthanum ions, similarly as chromium (1).

Temperature dependences of the EPR spectra of $Na_3La(PO_4)_2$ powder doped with 1 mol% Er and 0.4 mol% Cr allowed us to find additional information on magnetic properties of the compound.

The erbium EPR signal, visible at temperatures below 25 K, significantly varies its resonance position as a function of temperature. An effective spectroscopic factor g linearly modifies its value from g = 11.7 at 3.5 K to g = 8.7 at 25 K (Fig. 4a). Simultaneously, the intensity of this resonance line decreases as a function of temperature roughly fulfilling Curie-Weiss (C-W) law (Fig. 4b). More detailed analysis of this dependency allows us to find non-monotonic behavior of the fitted C-W equation, where characteristic parameter θ (C-W temperature) takes the value of θ = 2.6 K at temperature below 15 K, whereas at temperature above 15 K we have obtained best fitting for θ = 10 K. This variation is better observed in Fig. 5a, presenting a reciprocal intensity of an EPR signal as a function of temperature. Additionally, at a temperature of 15 K we can observe a significant change of the width of this line (Fig. 5b). Layered structure of paramagnetic ions in the analyzed compound may be one of the possible explanations of this phenomenon [31].

The EPR signal detected in the magnetic field range of 150 to 450 mT, containing a group of resonance lines, is ascribed to chromium magnetic centers, gadolinium uncontrolled dopant and to a quartz pipe. All these lines are observed up to room temperature. Due to a small EPR signal (low EPR signal/bias ratio), we analyzed the chromium spectrum only in a range below 50 K, although it was detected at temperatures up to 225 K.

The all components of this signal are located around a position with g ≈ 1.96 to 1.99. Chromium ions in the lanthanum orthophosphates may occupy the positions of lanthanum, that are surrounded by six oxygen ions. Due to a large difference in ionic radii between La^{3+} (132 pm), Gd^{3+} (120 pm) and Cr^{3+} (75.5 pm) one can expect that the environment of chromium Cr^{3+} ion deviates from an ideal octahedral geometry. It leads to an increase in value of D parameter (zero field splitting) and higher splitting of the EPR spectra (a range of magnetic field between 150 mT and 450 mT).

Fig. 6a (points) shows an integral intensity of the chromium (1) signal as a function of temperature. The solid line reveals C-W relation. As one can see C-W temperature equals to θ = 1.9 K, indicating low ferromagnetic interactions. But the dependence of the product of the integral intensity and temperature, proportional to a square of magnetic moment, reveals ferromagnetic like interaction only below 15 K, while over this temperature, antiferromagnetic like interaction begins. The position of the resonance line, g, reveals some shifting versus temperature, increasing from 1.96 at liquid helium temperature up to 1.995 at 225 K (Fig. 6b). Fig 7 presents temperature dependence of the reciprocal intensity and the linewidth of chromium (1) signal, respectively. From Fig. 7a it can be seen that weak ferromagnetic interactions dominate between chromium (1) ions. The linewidth (Fig. 7b) decreases exponentially with increasing

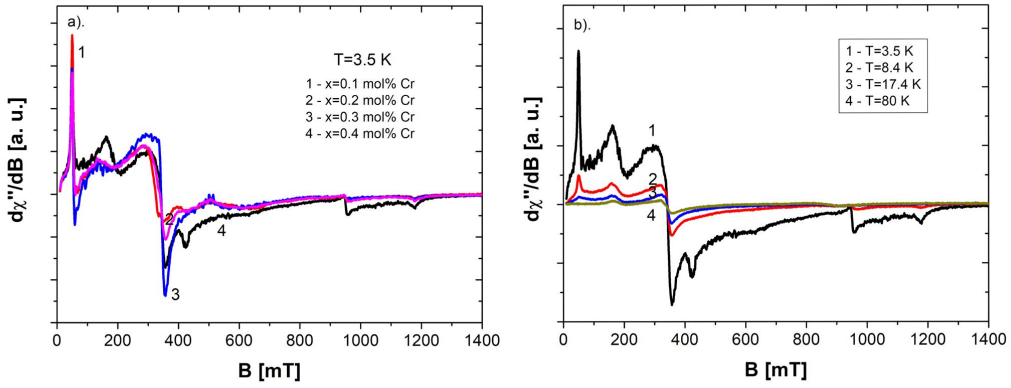

Fig. 2. (a) EPR spectra of the $Na_3La_{0.99-x}Er_{0.01}Cr_x(PO_4)_2$, x = 0.001 – 0.004 at T = 3.5 K, (b) temperature dependence of the EPR spectra.

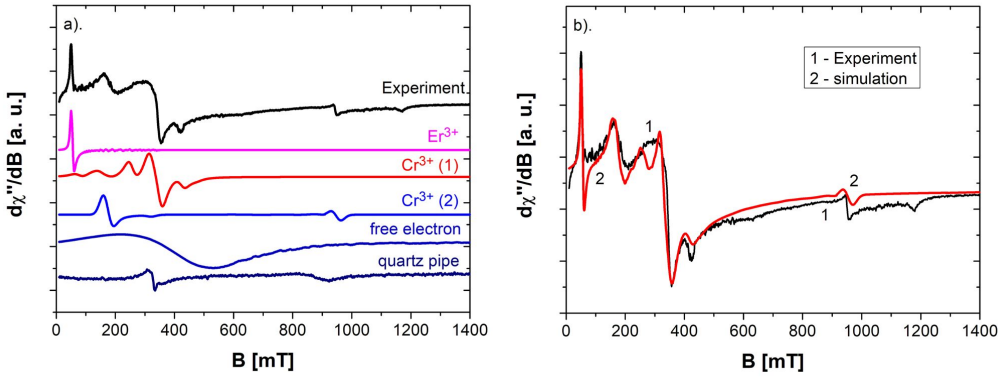

Fig. 3. (a) experimental EPR spectrum of the $Na_3La(PO_4)_2$ doped with 1 mol% Er and 0.4 mol% Cr and paramagnetic signals originating from Er^{3+}, Cr^{3+} (1), Cr^{3+} (2), Gd^{3+} and a quartz pipe contributing to it, (b) experimental EPR spectrum (1) and simulated one (2) being a superposition of the signals presented in Fig. 2a.

temperature indicating shortening of the lattice relaxation time.

EPR spectra of the $Na_3La(PO_4)_2$ powder doped with 1 mol% of Er and 0.4 mol% of Cr contain additionally some bands assigned to chromium (2) center. The signal preserves its position in magnetic field with $g \sim 3.74$. It is detectable at a temperature up to 225 K. The integral intensity of the EPR spectrum vs. temperature fulfills C-W law with C-W temperature equal to about $\theta \sim 2.73$ K, indicating low ferromagnetic interactions between chromium (2) ions (Fig. 8a), similarly as chromium (1) center. But the law is fulfilled only below 10 K, similarly as in the case of erbium center. It could be assigned to Cr^{3+} ions at sodium lattice positions or interstitials. The difference between other parameters of the chromium (2) EPR line below and above 10 K can be observed also in Fig. 8b and Fig. 9b, presenting the reciprocal intensity and a width of the line as a function of temperature, respectively. The most interesting feature is shown in Fig. 9b, where a product of an integral intensity and temperature

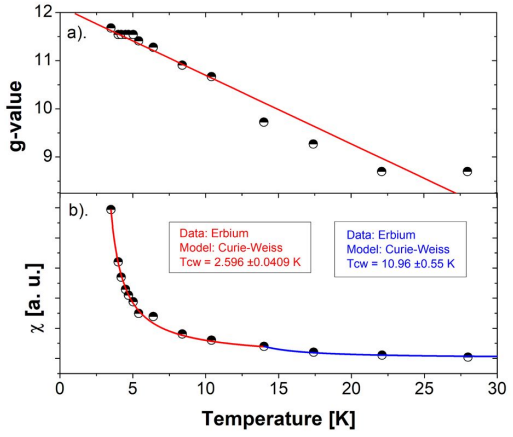

Fig. 4. (a) position of erbium EPR resonance line of $Na_3La(PO_4)_2$ powder doped with 1 mol of Er and 0.4 mol% of Cr, (b) integral intensity of the low-field erbium signal; solid lines reflect C-W dependence.

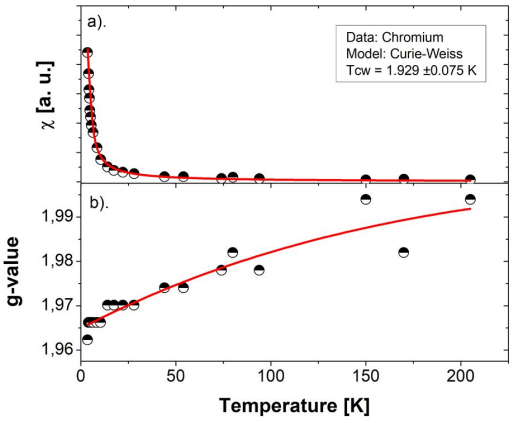

Fig. 6. (a) integral intensity of the chromium (1) EPR signal (points) vs. temperature (solid line reflects C-W dependence, (b) position of the resonance EPR line vs. temperature.

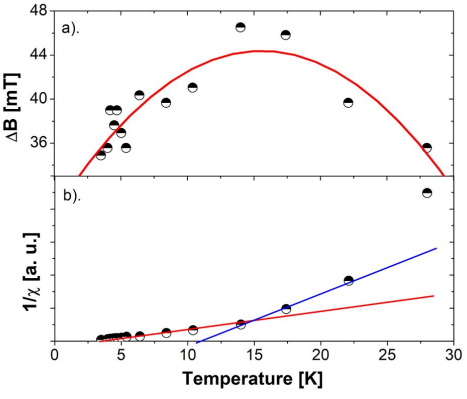

Fig. 5. (a) reciprocal of low field erbium EPR integral intensity of $Na_3La(PO_4)_2$ powder doped with 1mol% of Er and 0.4 mol% of Cr, (b) the linewidth of the low field erbium signal; the solid line shows only the tendency.

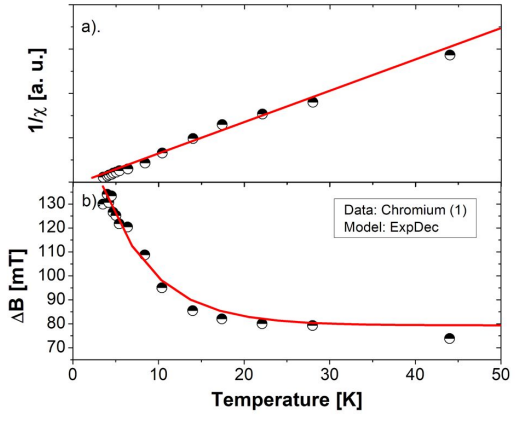

Fig. 7. (a) reciprocal of integral intensity of chromium (1) signal vs. temperature, (b) linewidth of the chromium (1) signal vs. temperature.

vs. temperature is presented. The variation of the slope of such a curve indicates a type of dominating magnetic interaction. The slope reveals domination of ferromagnetic interactions at temperatures below 5 K and over 15 K, whereas in the range between 5 K and 15 K, antiferromagnetic interactions prevail among responsible magnetic centers.

From the above considerations it results that both erbium and some part of chromium ions (chromium (1)) substitute for lanthanum ions but the sites reveal different coordination number and distortion. Independently of a type of dopant, some kind of structural or magnetic rearrangement takes place in a temperature range of 10 K to 15 K, leading to a change in a strength of magnetic interactions (erbium) or a change in a kind of the interactions (chromium (2)).

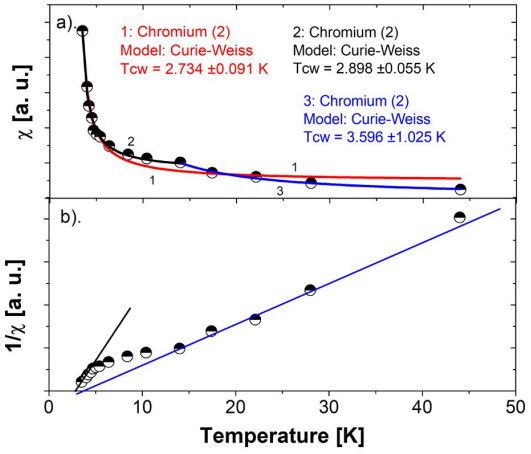

Fig. 8. (a) integral intensity of the chromium (2) EPR signal vs. temperature, (b) reciprocal of an integral intensity of the chromium (2) EPR signal vs. temperature.

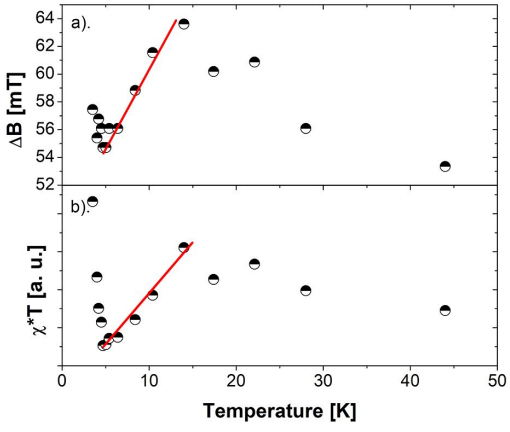

Fig. 9. (a) linewidth of the chromium (2) EPR signal vs. temperature, (b) the product of an integral intensity and temperature for the chromium (2) EPR signal.

3.2. Magnetic susceptibility results

As one can see from Fig. 10, magnetic susceptibility of the $Na_3La(PO_4)_2$ sample doped with 1 mol% of Er and 0.4 mol% of Cr, reveals C-W behavior with C-W temperature varied from ~ -0.84 K to -2.27 K. It suggests dominating antiferromagnetic type of magnetic interactions in the compound. The discrepancy between EPR and magnetic susceptibility measurements can be explained by the fact that EPR measurements, contrary to magnetic susceptibility, do not detect all paramagnetic ions in the investigated compounds. Moreover, some of the magnetic interactions observed in the EPR experiment may be due to short living magnetic complexes, that could not be detected by magnetic susceptibility measurements. Both, EPR and magnetic susceptibilities, reveal weak magnetic interactions which could be interpreted also as lack of such interactions.

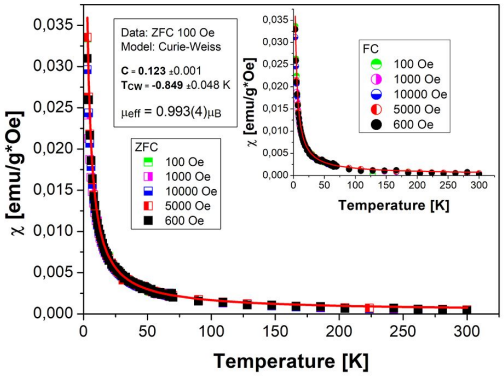

Fig. 10. Magnetic susceptibility of the $Na_3La(PO_4)_2$ sample doped with 1 mol% of Er and 0.4 mol% of Cr versus temperature for two regimes: ZFC and FC (inset), and magnetic fields from 100 Oe up to 10.000 Oe.

We have calculated a theoretical value of an effective magnetic moment of the $Na_3La(PO_4)_2$ sample doped with 1 mol% of Er and 0.4 mol% of Cr according to the following equation [41]:

$$\mu_{eff} = \sqrt{x \cdot \mu_{eff1}^2 + (1-x) \cdot \mu_{eff2}^2}, \qquad (1)$$

where: x – Er content, and, $\mu_{eff1,2}$ – effective magnetic moments of free ions (9.5 μ_B for Er, and 3.87 μ_B for Cr (S = 3/2, L = 0), μ_B – Bohr magneton). The theoretical value is equal to 0.990 μ_B. The effective magnetic moment calculated from magnetic susceptibility measurements is equal to $\mu_{eff} = 0.993$ μ_B for the magnetic field of 100 Oe (inset in Fig. 10). This value grows with

an increase in the magnetic field value. For the magnetic field of 10.000 Oe it reaches the value of $\mu_{eff} = 1.09\ \mu_B$. The differences of the effective magnetic moments between ZFC and FC modes are within measurement error. It seems that only erbium and chromium ions contribute to the value.

4. Magnetic properties of $Na_3Gd_{0.99-x}Er_{0.01}Cr_x(PO_4)_2$: x = 0.001 to 0.004

4.1. EPR results

In the EPR spectra of Gd^{3+} ions with f shell filled with seven electrons (ground state $^8S_{7/2}$), one can expect seven well resolved lines originating from its fine structure. Usually, EPR spectra of Gd^{3+} ions are composed of the main broad asymmetric line with unresolved structure, centred at g $\sim$ 2 and additional unresolved lines located at lower (g $\sim$ 6) and higher (g $\sim$ 1.5) magnetic fields. EPR spectrum of individual powder should be considered as an envelope of unresolved anisotropic fine structure of Gd^{3+} ions, centered at g $\sim$ 2. The intensity of erbium EPR line is lower than that of gadolinium, so erbium ions can only be distinguished at low temperatures. Considering the background signal originating from the gadolinium ions one may conclude that the appearance of the erbium signals in the EPR experimental spectra of these compounds may be difficult or impossible to notice. The same concerns chromium ions. The intensity of the EPR signal (the area under an absorption curve) registered for the $Na_3Gd_{0.99-x}Er_{0.01}Cr_x(PO_4)_2$: x = 0.001 to 0.004 compounds (Fig. 11) is at least two orders of magnitude higher than the intensity of uncontrolled Gd^{3+} centers detected for $Na_3La_{0.99-x}Er_{0.01}Cr_x(PO_4)_2$: x = 0.004.

As one can see from Fig. 11, the intensity of the EPR signal increases when the concentration of chromium dopants lowers which is an anticipated result. The broad EPR spectrum, centered at g $\sim$ 2, originates from Gd^{3+} ions. The EPR signal of erbium and chromium ions is not recognizable in the experimental spectra. EPR spectrum of

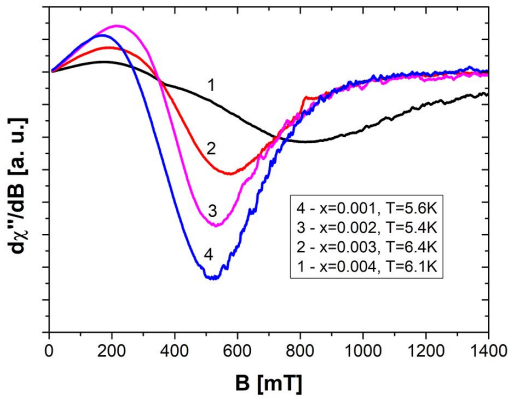

Fig. 11. EPR spectra of the $Na_3Gd_{0.99-x}Er_{0.01}Cr_x(PO_4)_2$: x = 0.001 to 0.004 compounds at a temperature of $\sim$6 K.

the $Na_3Gd_{0.99-x}Er_{0.01}Cr_x(PO_4)_2$ compound highly doped with chromium, appears to be a superposition of at least two Gd centers. It is clearly observed only at temperatures lower than 6 K. One of the reasons of such observation can be different distances between gadolinium ions in $Na_3Gd(PO_4)_2$ structure.

In Fig. 12 EPR spectra of the $Na_3Gd_{0.99-x}Er_{0.01}Cr_x(PO_4)_2$: x = 0.001 to 0.004 compounds for several temperatures are presented. All the spectra are close each other, excluding the one registered for the compound with higher concentration of chromium ions. The shape of all the lines is asymmetric suggesting some anisotropy of magnetic properties of the compounds. To find additional information on a second kind of Gd center, we deconvoluted the EPR lines registered at temperatures lower than 6 K, using Lorentzian lineshapes. The latter provided better results than the modified Bloch or Landau-Lifshitz lineshapes. We have obtained satisfactory results for two Lorentzian lineshapes, that could represent two kinds of paramagnetic Gd centers, magnetically inequivalent.

From the deconvolution of an EPR line of the $Na_3Gd_{0.99-x}Er_{0.01}Cr_x(PO_4)_2$: x = 0.004 compound, detected at 5.63 K, we have found that at the temperature an overall EPR shape of the line is a superposition of at least two wide line-shapes, centered at g $\sim$ 2.28 and g $\sim$ 1.65. The positions of

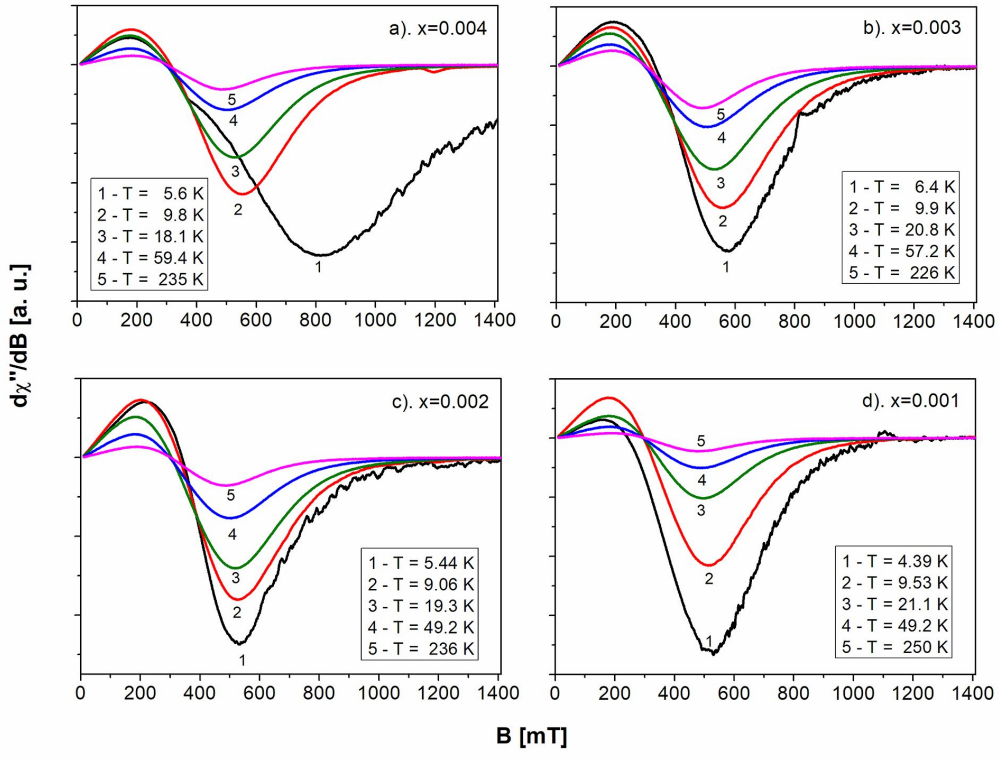

Fig. 12. EPR spectra of the $Na_3Gd_{0.99-x}Er_{0.01}Cr_x(PO_4)_2$: x = 0.004 to 0.001 compounds for several temperatures.

both lines change with a temperature variation and reach g $\sim$ 2 at about 25 K. Clear separation of the two lines is observed only at chromium concentration higher than 0.2 mol.%, as it could be seen in Fig. 13, where the position of resonance EPR lines, g, is plotted vs. temperature for all of the investigated compounds.

A shift of the EPR resonance line position along with temperature observed for low temperatures may be due to the presence in the compound some internal magnetic fields, resulting from, e.g., interlinear interactions of gadolinium ions or complex gadolinium ordering (different distances between gadolinium ions).

In Fig. 14 integral intensities of the EPR spectra are presented for all of the investigated sodium gadolinium phosphates. We have obtained enough good approximation to experimental points using Bleaney-Bowers equation adopted to ions with a spin S = 7/2 [42]. From the figure one can see that gadolinium ions are well isolated (very low value of exchange interaction, J). Moreover, magnetic interactions inside these compounds are weak, antiferromagnetic like, with C-W temperature not exceeding -1 K.

4.2. The results of magnetic susceptibility measurements

In Fig. 15 one can see the results of magnetic susceptibility measurements (FC mode) recorded for the $Na_3Gd_{0.99-x}Er_{0.01}Cr_x(PO_4)_2$: x = 0.001 sample at magnetic fields varying from 100 Oe to 10.000 Oe. In this range of magnetic field, T_{cw} – Curie-Weiss temperature is low and negative one (-0.40 K to -1.13 K), indicating dominance of low antiferromagnetic interactions. This

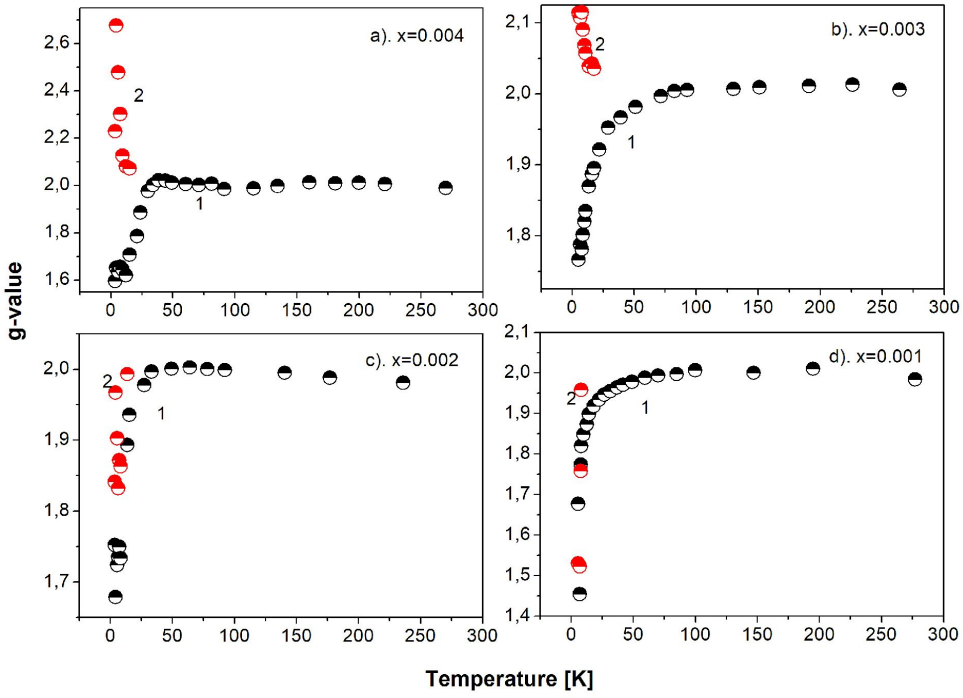

Fig. 13. Position of the EPR resonance lines, g, calculated for the $Na_3Gd_{0.99-x}Er_{0.01}Cr_x(PO_4)_2$: x = 0.004 to 0.001 compounds.

result remains in a good agreement with EPR measurements. We have calculated a theoretical value of an effective magnetic moment for the $Na_3Gd_{0.99-x}Er_{0.01}Cr_x(PO_4)_2$: x = 0.004 and $Na_3Gd_{0.99-x}Er_{0.01}Cr_x(PO_4)_2$: x = 0.003 samples according to equation 1. This equation was developed to take into account three paramagnetic ions: Gd^{3+}, Er^{3+}, Cr^{3+}.

From the magnetic susceptibility measurements it results that the effective magnetic moment grows with increasing magnetic field. For the lowest magnetic field (ZFC 100 Oe) it is equal to $\mu_{eff} = 8.052\ \mu_B$, which corresponds to the theoretical value of the total magnetic moment (free ions). For higher magnetic fields it reaches a value of $\mu_{eff} = 8.375(4)\ \mu_B$. For the FC mode, the value of the effective magnetic moment changes from $\mu_{eff} = 7.985(3)\ \mu_B$ to $\mu_{eff} = 8.378(4)\ \mu_B$, respectively, as is shown in Fig. 15. Small discrepancy between the values of effective magnetic moments calculated at ZFC and FC modes at low magnetic fields can be attributed to low anisotropy of paramagnetic ions. This anisotropy disappears with increasing magnetic field which may indicate a strong crystal field around the paramagnetic ions. In the $NaLa(PO_4)_2$ compound we have not observed such significant difference between effective magnetic moments calculated for ZFC and FC modes. It may indicate that the strength of crystal field depends on a type and ionic radius of a dopant with respect to substituted lattice ion. In the inset of Fig. 15 one can see also the dependence of T_{CW} on magnetic field. From the dependence it results that antiferromagnetic interactions strength (proportional to T_{CW}) grows with value of magnetic field.

5. Discussion and conclusions

Both, erbium and chromium ions, are clearly observed in the EPR spectrum of the $Na_3La(PO_4)_2$ powders doubly doped with Er^{3+} and Cr^{3+}.

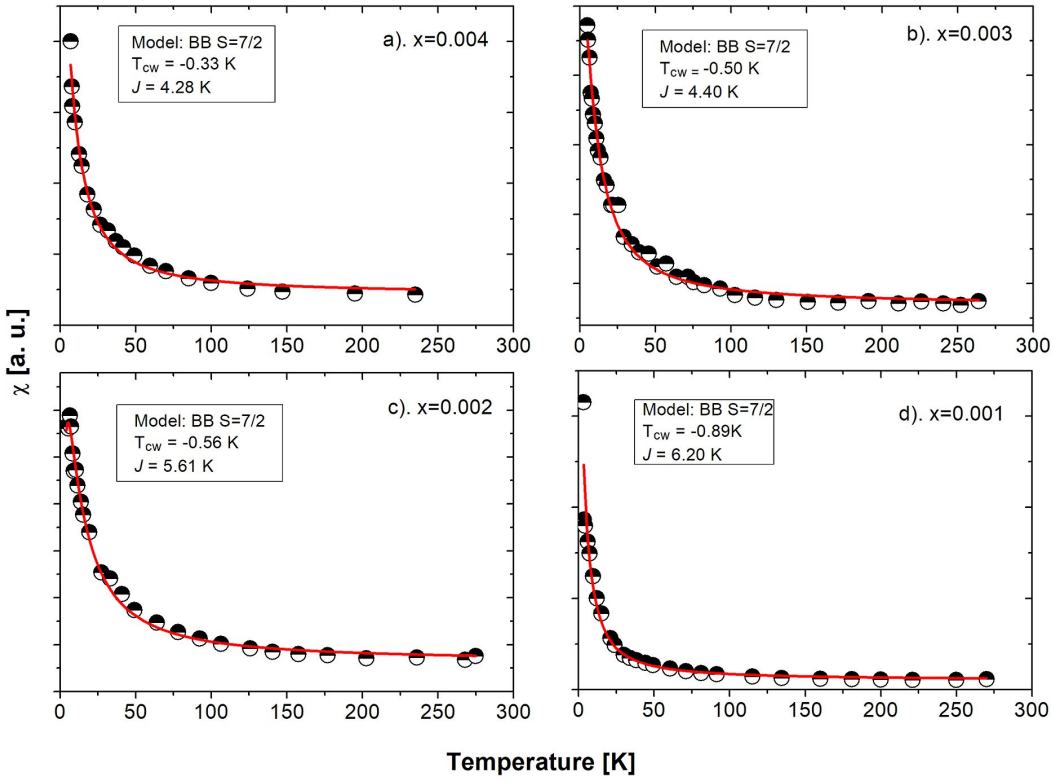

Fig. 14. Temperature dependence of the EPR integral intensity calculated for $Na_3Gd_{0.99-x}Er_{0.01}Cr_x(PO_4)_2$: x = 0.001 to 0.004 powders. Solid lines reflect the fitting of calculated EPR integral intensity to the Bleaney-Bowers (BB) equation adopted for ions with a spin S = 7/2 [42].

In contradiction to this, the same kind of doping does not result in the presence of clear EPR signals in doubly doped $Na_3Gd(PO_4)_2$ powder. It is due to a high intensity of a wide gadolinium EPR spectrum, which has asymmetric shape, indicating a large magnetic anisotropy of the compound. Unexpectedly, this gadolinium EPR signal does not manifest itself in large antiferromagnetic interactions, characteristic of magnetically dense gadolinium compounds. C-W temperature calculated both from EPR and magnetic susceptibility measurements, does not exceed -1 K, which indicates low antiferromagnetic interactions between paramagnetic ions in the $Na_3Gd(PO_4)_2$:Er, Cr powder. The above supposition confirms also low values of magnetic exchange constant, J. The effective magnetic moment does not exceed the value characteristic of gadolinium free ions, so mainly gadolinium ions contribute to its value. Nevertheless, doping the $Na_3Gd(PO_4)_2$ powder with erbium and chromium ions affects shapes of the EPR spectra, revealing two positions of gadolinium ions in the $Na_3Gd(PO_4)_2$ lattice, fixed by value of g-factor: $g \sim 2$ and $g \sim 1.65$ at T = 5.6 K. The EPR resonance lines positions vary along with temperature in a low temperature range (below 25 K), which suggests the presence of some internal magnetic fields in the compound, being an effect of complex (1D, 2D) magnetic interactions.

EPR spectra of $Na_3La(PO_4)_2$ powders doped with Er^{3+} and Cr^{3+} reveal presence of erbium (S = 1/2) and chromium (S = 3/2) ions, but the latter appear in two different lattice positions.

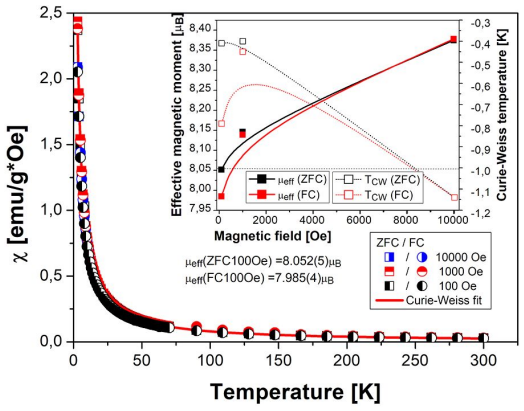

Fig. 15. Magnetic susceptibility (ZFC and FC mode) of the $Na_3Gd_{0.99-x}Er_{0.01}Cr_x(PO_4)_2$: x = 0.004 sample vs. temperature, recorded for magnetic fields:100, 1000 and 10.000 Oe. Inset presents μ_{eff}(H) and T_{CW}(H) dependences.

First of them is the lanthanum lattice ion position ($g_{eff} \sim 1.99$) and the second one is the sodium or interstitial position ($g \sim 3.74$). Taking into account ionic radii of Cr^{3+} and Na^+ ions, such a substitution is possible, but due to necessity of charge compensation it leads to a significant change of resonance conditions as compared to Cr^{3+} ions occupying the lanthanum sites. This is the reason why the EPR signal takes also high field positions. From the intensity of EPR signal one can conclude that the number of chromium ions occupying the latter position is twice lower. Both kinds of chromium ions reveal low ferromagnetic interaction (C-W temperature ∼2 K).

The resonance positions of EPR lines registered for Er^{3+} and Cr^{3+} at lanthanum positions, characterized by g-values, vary along with temperature, linearly decreasing for the former, and increasing for the latter. The behavior may be due to the presence of internal magnetic fields in the $Na_3La(PO_4)_2$ powders. This conclusion is coincident with the one derived for $Na_3Gd(PO_4)_2$ powder. Behavior of the reciprocal of integral EPR intensity, product of the integral intensity and temperature, as well as a linewidth vs. temperature calculated for erbium and chromium (2) ions, suggest rearrangement of the ions in a temperature range of 10 K to 15 K. In the case of erbium signal (g = 11.7 at 3.5 K), C-W temperature is as high as ∼2 K below the temperature range, while it grows to ∼10 K above this range. The evolving of the strength of magnetic interactions in the temperature range of 10 K to 15 K could be assigned to competition between linear (1D – chains) and inter-linear (2D) magnetic interactions of the ions. With decreasing temperature and lowering the lattice vibration intensity, additional antiferromagnetic interactions between the chains take place, leading to weakening of the effective interactions between the ions.

Magnetic susceptibility measurements confirm a weak magnetic interaction in erbium and chromium doped $Na_3La(PO_4)_2$ powder. They reveal an antiferromagnetic kind of magnetic interactions with C-W temperature as high as ~ -2 K.

Acknowledgements

This work was supported by the Polish Ministry of Science and Higher Education in the frame of the grant No. N N209 767240.

References

[1] LETHO J.Z., HOUNEOU P., EHOLIE R.C.R., *C. R. Acad. Sci. (Paris) ser. II*, 307 (1988), 1177.
[2] KLOSS M., FINKE B., SCHWARZ L., HABERLAND D., *J. Lumin.*, 72 – 74 (1997), 684.
[3] SCHWARZ L., KLOSS M., ROHMAN A., SASUM U., HABERLAND D., *J. Alloy. Compd.*, 275-277 (1998), 93.
[4] KLOSS M., SCHWARZ L., HÖLSA J.P.K., *Acta Phys. Pol. A,* 95 (1999), 343.
[5] MOROZOV V.A., BOBYLEV A.P., GERASIMOVA N.V., KIRICHENKO A.N., MIKHAILIN V.V., PUSHKINA G.YA., LAZORYAK B.I., KOMISSAROVA L.N., *Russ. J. Inorg. Chem.*, 46 (2001), 711.
[6] PARREU I., SOLE R., GAVALDA J., MASSONS J., DIAZ F., AGUILO M., *Chem. Mater.*, 15 (2003), 5059.
[7] LU C.-H. GODBOLE S.V., *J. Mater. Res.*, 19 (2004), 2336.
[8] GUZIK M., AITASALO T., SZUSZKIEWICZ W., HÖLSA J., KELLER B., LEGENDZIEWICZ J., *J. Alloy. Compd.,* 380 (2004), 368.
[9] LIANG H.B., TAO Y., SU Q., *Mater. Sci. Eng. B-Solid*, 119 (2005), 152.
[10] BENARAFA L., RGHIOUI L., NEFFAR R., IDRISSI M.S., KNIDIRI M., LORRIAUX A., WALLART F., *Spectrochim. Acta A*, 61 (2005), 419.
[11] PARREAU I., CARVAJAL J.J., SOLANS X., DIAZ F., AGUILO M., *Chem. Matter.*, 18 (2006), 221.
[12] FANG M., CHENG W.D., ZHANG H., ZHAO D., ZHANG W.L., YANG S.L., *J. Solid State Chem.*, 181 (2008), 2165.

[13] HASHIMOTO N., TAKADA Y., SATO K., IBUKI S., *J. Lumin*., 48 (1991), 893.
[14] OTSUKA K., MIYAZAWA S., YAMADA T., IWASAKI H., NAKANO J., *J. Appl. Phys.*, 48 (1977), 2099.
[15] CHEVALIER J., GREMILLARD L., *J. Eur. Ceram. Soc*., 29 (2009), 1245.
[16] MOORE P.B., *Am. Mineral*., 58 (1973), 32.
[17] GODLEWSKA P., BANDROWSKI SZ., MACALIK L., LISIECKI R., RYBA-ROMANOWSKI W., SZCZYGIEŁ I., ROPUSZYŃSKA-ROBAK P., HANUZA J., *Opt. Mater*., 34 (2012), 1023.
[18] AITASALO T., GUZIK M., SZUSZKIEWICZ W., HOLSA J., KELLER B., LEGENDZIEWICZ J., *J. Alloy. Compd*., 380 (2004), 405.
[19] LEGENDZIEWICZ J., GUZIK M., CYBINSKA J., STEFAN A., LUPEI V., *Opt. Mater*., 30 (2008), 1667.
[20] LEGENDZIEWICZ J., GUZIK M., CYBINSKA J., *Opt. Mater*., 31 (2009), 567.
[21] LEGENDZIEWICZ J., CYBINSKA J., GUZIK M., BOULON G., MEYER G., *Opt. Mater*., 30 (2008), 1655.
[22] LEGENDZIEWICZ J., GUZIK M., SZUSZKIEWICZ W., *J. Alloy. Compd*., 451 (2008), 165.
[23] SZUSZKIEWICZ W., KELLER B., GUZIK M., AITASALO T., KIITTYKOSKI J., HOLSA J., LEGENDZIEWICZ J., *J. Alloy. Compd*., 341 (2002), 297.
[24] GUZIK M., LEGENDZIEWICZ J., SZUSZKIEWICZ W., WALASEK A., *Z. Anorg. Allg. Chem*., 633 (2007), 310.
[25] LEGENDZIEWICZ J., GUZIK M., CYBINSKA J., STEFAN A., LUPEI V., *J. Alloy. Compd*., 451 (2008), 158.
[26] SZULIA S., KOSMOWSKA M., KOŁODZIEJ H.A., SOBCZYK M., CZUPINSKA G., *J. Mol. Struct*., 1006 (2011), 409.
[27] SZULIA S., KOŁODZIEJ H.A., SZUSZKIEWICZ W., CZUPINSKA G., *J. Non-Cryst. Solids,* 356 (2010), 805.
[28] PIOTROWSKA D., MATRASZEK A., SZULIA S., KOSMOWSKA M., SZCZYGIEŁ I., *J. Alloy. Compd*., 585 (2014), 337.
[29] FARMER J.M., BOATNER L.A., CHAKOUMAKOS B.C., RAWN C.J., MANDRUS D., JIN R., BRYAN J.C., *J. Alloy. Compd*., 588 (2014), 182.
[30] GUZIK M., LEGENDZIEWICZ J., SZUSZKIEWICZ W., WALASEK A., *Opt. Mater*., 29 (2007), 1225.
[31] MATRASZEK A., GODLEWSKA P., MACALIK L., HERMANOWICZ K., HANUZA J., SZCZYGIEŁ I., *J. Alloy. Compd*., 619 (2015), 275.
[32] MATRASZEK A., SZCZYGIEŁ I., *J. Therm. Anal. Calorim*., 93 (2008), 689.
[33] KARPOV O.G., PUSHCHAROVSKII D.Y., KHOYMAKOV A.P., POBEDIMSKAYA A.E., BELOV N.V., *Soviet Phys. Crystallogr*., 25 (1980), 650.
[34] KACZMAREK S.M., TSUBOI T., LENIEC A., NAKAI Y., LENIEC G., BERKOWSKI M., HUANG W., *J. Cryst. Growth,* 401 (2014), 828.
[35] SINGH V., CHAKRADHAR R.P.S., RAO J.L., KWAK H.-Y., *J. Mater. Sci*., 46 (2011), 2331.
[36] KHADDAR-ZINE S., GHORBEL A., NACCACHE C., *J. Mol. Catal. A-Chem.,* 150 (1999), 223.
[37] MOMBOURQUETTE M.J., WEIL J.A., MCGAVIN D.G., *EPR-NMR User's Manual,* University of Saskatchewan, Saskatoon, Canada, 1999.
[38] KRIPAL R., PANDEY S., *Spectrochim. Acta A,* 76 (2010), 62.
[39] BRAVO D., LOPEZ F.J., *Opt. Mater*., 13 (1999), 141.
[40] BUDIL D.E., PARK D.G., BURLITCH J.M., GERAY R.F., DIECKMANN R., FREED J.H., *J. Chem. Phys.,* 101 (1994), 3538.
[41] LUBINSKII N.N., BASHKIROV L.A., GALYAS A.I., SHEVCHENKO S.V., PETROV G.S., SIROTA I.M., *Inorg. Mater*., 44(9) (2008), 1015.
[42] LENIEC G., MACALIK L., KACZMAREK S.M., SKIBINSKI T., HANUZA J., *J. Mater. Res*., 27 (2012), 2973.

Received 2016-10-30
Accepted 2017-10-18